DOI: 10.1002/chem.200700435

Micelle-Induced Versatile Performance of Amphiphilic Intramolecular Charge-Transfer Fluorescent Molecular Sensors

Jiaobing Wang,[a, b] Xuhong Qian,*[a, b] Junhong Qian,[a] and Yufang Xu[a]

Abstract: A series of amphiphilic intramolecular charge-transfer fluorescent molecular sensors AS1–3, equipped with a rod-shaped hydrophobic 2-phenylbenzoxazole fluorophore and a hydrophilic tetraamide Hg^{2+}-ion receptor, have been prepared. These sensor molecules could be incorporated into the hydrophobic sodium dodecyl sulfate (SDS) micelle, which is confirmed by the clear spectral blue shift and emission enhancement observed at the critical micelle concentration of SDS. Systematic examination of the sensor–Hg^{2+} complexation, by using both UV/visible and fluorescence spectroscopy, indicates that SDS significantly modulates both the binding event and signal transformation of these sensor molecules. The potential advantages are fourfold: 1) SDS substantially increases the Hg^{2+}-ion association constant and results in an amplified sensitivity. 2) SDS initiates spectral features which facilitate Hg^{2+}-ion analysis, for example, in addition to the strengthened fluorescence of the free sensors AS1–3, the original "on–off" response of AS2 toward the Hg^{2+} ion is transformed into a self-calibrated two-wavelength ratiometric signal, while for AS3, Hg^{2+}-ion complexation in the presence of SDS results in a 180 nm blue shift, which is preferred to the 51 nm spectral shift obtained without SDS. 3) Thermoreversible tuning of the dynamic detection range is realized. 4) Highly specific Hg^{2+}-ion identification could be achieved by using the SDS-induced fingerprint emission (358 nm) of the AS2–Hg^{2+} complex. Altogether, this work demonstrates a convenient and powerful strategy that remarkably elevates the performance of a given fluorescent molecular sensor. It also implies that for a specific utilization, much attention should be paid to the microenvironment in which the sensor resides, as the behavior of the sensor might be different from that in the bulk solution.

Keywords: charge transfer · fluorescence · mercury · micelles · sensors

Introduction

Fluorescent molecular sensing has enjoyed intensive research over the years,[1] which is mainly driven by the fact that many fields, such as scientific research, industrial production, and our daily lives, require efficient analyte reporting. It is generally accepted that a small fluorescent sensor molecule (FSM), with its many inherent merits including high sensitivity, high specificity, and real-time in situ response, can provide a lot of crucial information for practical applications. Moreover, deep insight into the recognition and signal transduction processes at the molecular level will provide indispensable knowledge for the understanding of life phenomena.[2–4] Nonetheless, despite the fact that numerous pieces of research aimed at the development of novel FSMs have been performed and some basic principles governing the performance of a special FSM have been established, it is still challenging to create FSMs with desired properties. Under these circumstances, it will be invaluable to find ways that can remarkably elevate the performance of a given FSM.

Surfactant, a versatile amphiphilic molecular star, finds rather wide utilization in different fields. For instance, in the textile industry, surfactant is used to prevent dye aggregation and to facilitate pigmentation, while in the mining process surfactant can be exploited for the enrichment of the

[a] Dr. J. Wang, Prof. Dr. X. Qian, Dr. J. Qian, Prof. Dr. Y. Xu
State Key Laboratory of Bioreactor Engineering and
Shanghai Key Laboratory of Chemical Biology
School of Pharmacy
East China University of Science and Technology
Shanghai 200237 (China)
E-mail: xhqian@ecust.edu.cn

[b] Dr. J. Wang, Prof. Dr. X. Qian
State Key Laboratory of Fine Chemicals
Dalian University of Technology
Dalian 116012 (China)
Fax: (+86) 21-6425-2603

Supporting information for this article is available on the WWW under http://www.chemeurj.org/ or from the author.

sparsely distributed minerals. Although for different purposes, most of these utilizations benefit from the advantage that surfactant molecules can offer a special phase or microenvironment, such as a micelle, distinct from the bulk solution. These new microenvironments have been cleverly used for self-assembled nanoreactors[5] or for the template synthesis of novel mesoporous materials.[6] We reasoned that if a tailor-made small FSM could share the virtues that surfactants provide, then large-amplitude performance elevation may be realized.[7] As a proof-of-principle demonstration of this speculation, we report herein a series of amphiphilic intramolecular charge-transfer (ICT) FSMs. We found that 1) enhanced sensitivity, 2) desirable spectral changes including "on–off" to ratiometric signal transformation, 3) a thermocontrolled dynamic detection range, and 4) highly specific analyte identification by the fingerprint emission of an analyte-sensor complex could be achieved when sodium dodecyl sulfate (SDS) was added up to its critical micelle concentration (CMC).

We chose the ICT FSMs[1a,b] mainly based on the following two considerations: 1) environment sensitivity and 2) compact receptor–fluorophore integration. In detail, first, an ICT FSM generally contains a "push–pull" π-electron system, in which an electron-donating group (donor) is electronically conjugated with the electron-withdrawing group (acceptor). Upon photoexcitation, this kind of FSM will experience a strong ICT process from the donor to the acceptor, which results in an enlarged excited-state dipole moment. Such an excited state is very sensitive to the microenvironment in which the sensor resides. For example, polar protic solvent often results in a decreased fluorescence, which is problematic for practical utilization. Thus, the SDS micelle, with its decreased polarity inside,[8] should cause favorable fluorescence enhancement for the incorporated ICT FSM. Second, to effectively modulate the ICT process by analyte complexation, some key atoms of the receptor are often shared by the fluorophore. In this way, the receptor is directly infused into the fluorophore platform. Such a compact receptor–fluorophore integration may offer the receptor a chance to make use of the microenvironment of the micelle surface. Namely, micelle incorporation of the hydrophobic fluorophore can largely drag the closely attached hydrophilic receptor into the counterionic cloud, in which the local concentration of cationic analyte is boosted by electrostatic interaction.[9] As a result, the receptor catches the analyte more efficiently. The above two points stress that an ICT FSM has the potential to experience a remarkable performance enhancement by virtue of the microenvironment of a micelle, both inside and outside (Scheme 1).

Amphiphilic ICT sensors AS1–3 (for synthesis see Scheme 2) are constructed by incorporating a hydrophilic

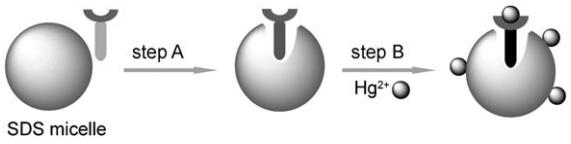

Scheme 1. Cartoon representation of the SDS micelle-assisted FSM performance enhancement. Step A: micelle incorporation modulates the ICT process. Step B: micelle functions as a "cation sponge".

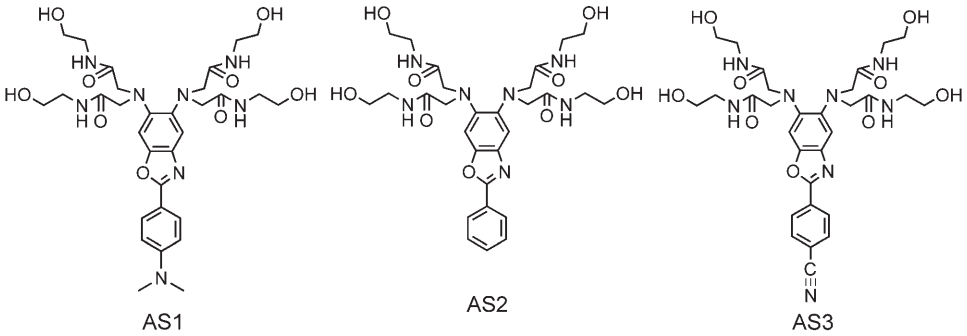

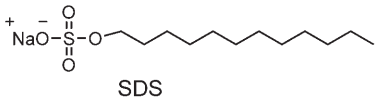

tetraamide Hg^{2+}-ion receptor[10] into a hydrophobic 2-phenylbenzoxazole fluorophore. Once the Hg^{2+} ion is caught by the receptor, π-electron conjugation within the fluorophore will be significantly perturbed and clear fluorescence signals (fluorescence quenching is also possible because of the heavy-atom effect) will be produced. The rod-shaped nonionic hydrophobic fluorophore would be compatible with the hydrocarbon tail of SDS and facilitates its incorporation into the SDS micelle. Moreover, different substituents on the *para* position of the 2-phenyl ring are introduced to modify the photophysical property and Hg^{2+} ion binding strength of AS1–3. The detailed synthesis of these sensors is provided in the Experimental Section.

Results and Discussion

UV/visible absorption and fluorescence spectra of free sensors AS1–3: As shown in Figure 1a, in neutral water solution AS1 shows a strong absorption band centered at 363 nm ($\varepsilon = 43\,400\ M^{-1}\,cm^{-1}$), whereas AS2 and AS3 both display two major bands, similar to each other in terms of band shape and molar absorption coefficient. The absorption of AS3 (366 nm, $\varepsilon = 18\,300\ M^{-1}\,cm^{-1}$; 256 nm, $\varepsilon = 25\,400\ M^{-1}\,cm^{-1}$) is found at a longer wavelength than that of

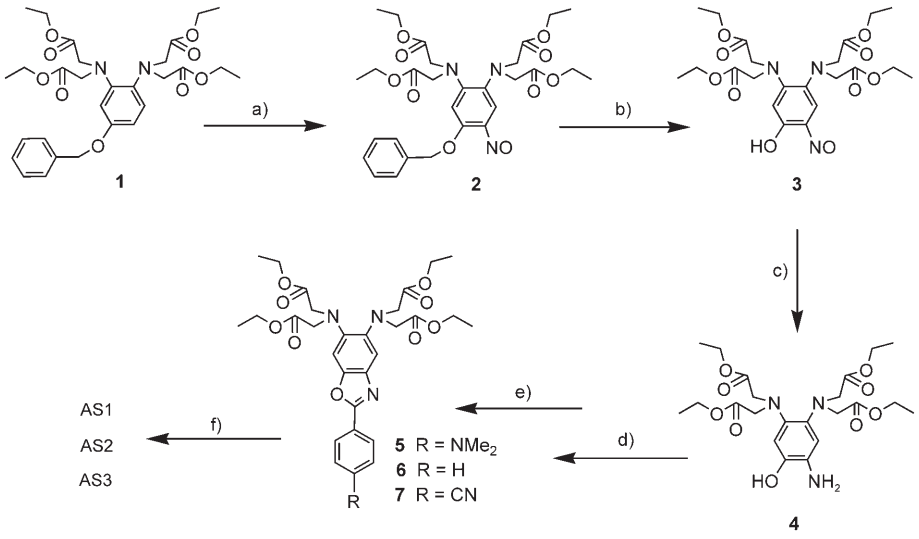

Scheme 2. Synthesis of sensors AS1–3: a) $NaNO_2$, CH_3COOH, 25 °C, 15 min, 98 %; b) Pd/C (5 wt %), cyclohexene, THF, reflux, 2 h, 96 %; c) Zn, CH_3COOH, 25 °C, 5 min; d) aromatic aldehyde, CH_2Cl_2, 35 °C, 10 min; e) $BaMnO_4$, benzene, reflux, 20 min, ≈50 %; f) 2-aminoethanol, CH_3CN, reflux, 2 h, ≈84 %.

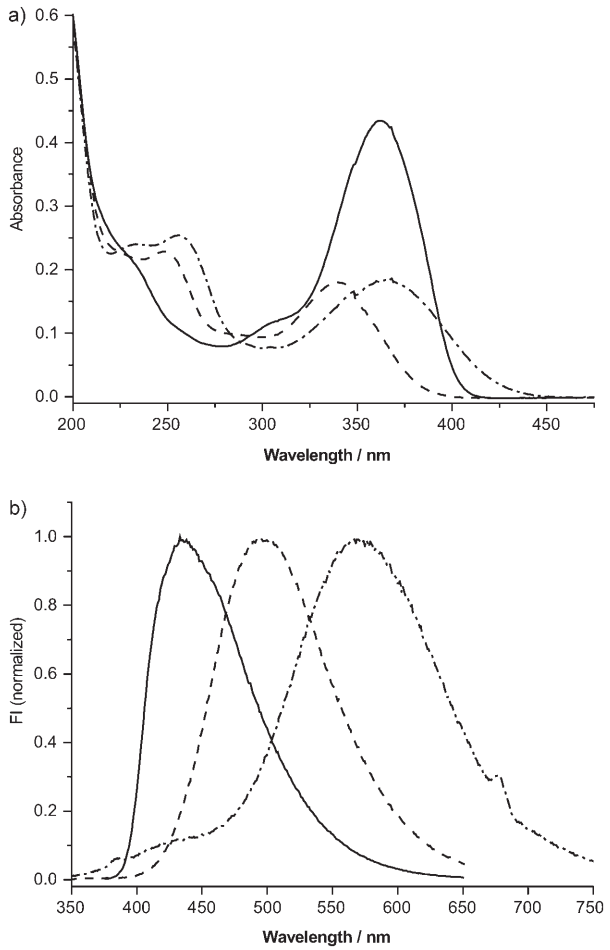

Figure 1. a) Absorption and b) normalized fluorescence spectra of sensors AS1–3 (10 μM) in neutral water solution. Excitation of AS1–3 was at 359, 320, and 339 nm, respectively. FI: fluorescence intensity, ——: AS1, - - - -: AS2, –•–•–: AS3.

AS2 (340 nm, $\varepsilon = 18000\,M^{-1}\,cm^{-1}$; 248 nm, $\varepsilon = 22800\,M^{-1}\,cm^{-1}$). This is caused by the electron-deficient cyanide group, which enhances π-electron push–pull interactions. Remarkably, the absorption of AS1 is different from that of AS2 and AS3. This observation could be ascribed to the different electronic configurations of sensors AS1–3. In detail, AS1 is no longer a simple sensor with D–A (D: electron donor, 5,6-diamino nitrogen atoms; A: electron acceptor, oxazole ring) constitution but a $D–A–D_1$ one.[11,12] If the D–A constitution is authentic, the electron-donating dimethylamino group should just play the "minor role" of tuning the electron density of the electron-acceptor moiety, as the cyanide group does on AS3, and a similar but blue-shifted absorption spectrum for AS1 should have been observed. However, in the $D–A–D_1$ system, the dimethylamino group acts as another electron donor D_1 and results in the absorption of the $D_1 \rightarrow A$[13] electron transition overlapping that of the $D \rightarrow A$ transition, thus giving the strong absorption band at 363 nm.

Sensors AS1–3 exhibit different emission colors (Figure 2b) ranging from blue (AS1, $\lambda_{em} = 436$ nm), via light green (AS2, $\lambda_{em} = 497$ nm), to deep orange (AS3, $\lambda_{em} = 576$ nm). Their fluorescence quantum yields (Φ) are determined to be 0.50, 0.48, and 0.067, respectively.[14] Clearly, AS1 is the brightest sensor molecule due to its large molar absorption coefficient and high fluorescence quantum yield. The comparatively weak emission of AS3 is not surprising considering its inherent, strong push–pull π-electron configuration because the intensive dipole moment, generated by photoexcitation, will result in a higher electron density on the oxazole nitrogen atom, which turns on new fluorescence deactivation pathways, such as enhanced hydrogen bonding with water molecules.[1a,b]

SDS effects on free sensors AS1–3: We next examined the SDS-induced spectral changes of sensors AS1–3 (Figure 2) in neutral aqueous solution. Generally speaking, 1) a clear spectral blue shift and emission enhancement were observed for all sensors and 2) steep transformations were found at the CMC (8.2 mM)[8] of SDS (Figure 2, insets). When 12 mM SDS[15] was present, fluorescence enhancement rates of 20 ($\Phi = 0.60$), 43 ($\Phi = 0.69$), and 176 % ($\Phi = 0.185$), accompanying emission blue shifts of 16, 20, and 18 nm, were achieved for sensors AS1–3, respectively. These results indicated that the hydrophobic fluorophore was successfully incorporated into the SDS micelle. In contrast to the emission

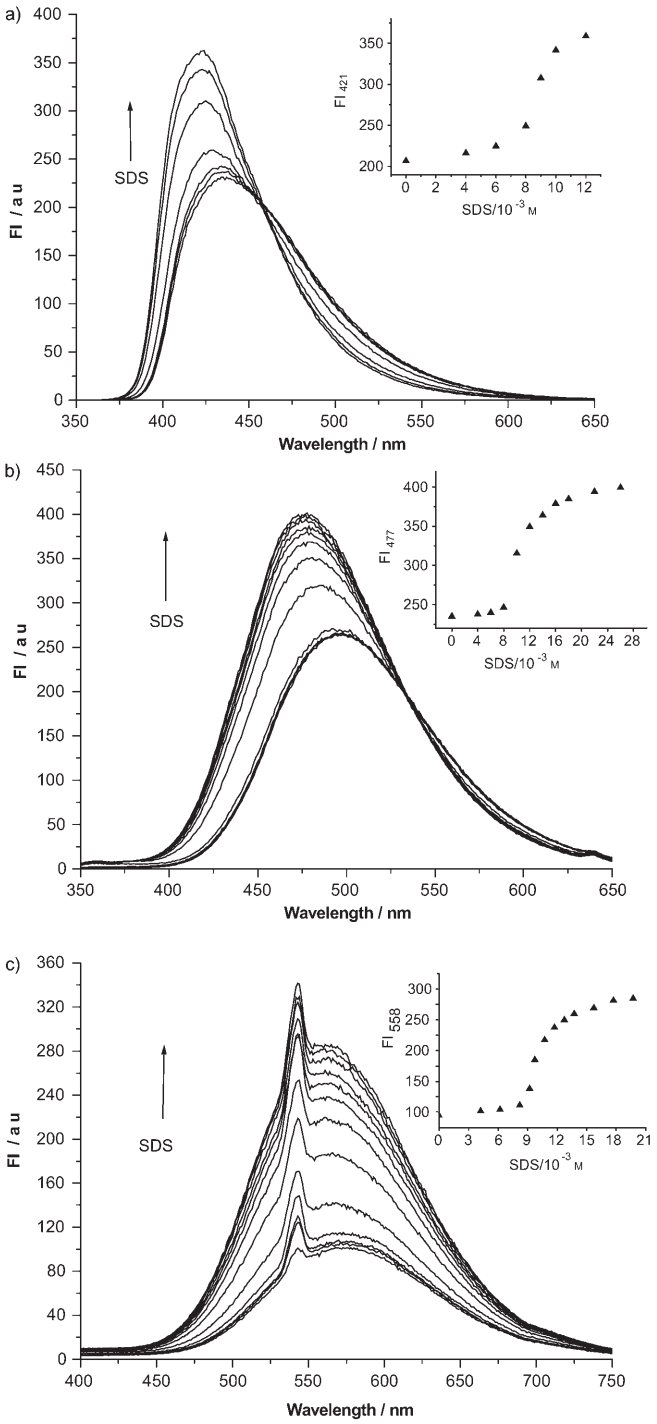

Figure 2. Fluorescence spectra of sensors (10 μM) a) AS1, b) AS2, and c) AS3 (peak at 540 nm is caused by Rayleigh scattering) in neutral water solution (pH 7.1, 25 °C) containing different concentrations of SDS. Excitation of AS1–3 was at 354, 320, and 270 nm, respectively, which was the isosbestic point on the absorption spectra. Inset: fluorescence intensity as a function of SDS concentration.

spectra, SDS only induced small spectral changes in the UV/visible absorption of AS1–3 (see the Supporting Information), indicating that the weaker dipole moment of the ground state is less sensitive to the polarity of the environment.

UV/visible responses on Hg^{2+}-ion titration: The UV/visible absorptions of AS1–3 all displayed clear spectral responses upon Hg^{2+}-ion[16] titration, indicating that complexation occurred both in the absence and presence of SDS. Distinctly, from these responses, three major features could be abstracted (Table 1). First, the UV/visible responses of AS1

Table 1. Summarized maximum absorption wavelength [nm] and molar absorption coefficient [$M^{-1}cm^{-1}$] of AS1–3 (10 μM) in the absence or presence of the Hg^{2+} ion (20 μM) and SDS (12 mM).

Sensor	λ Free	λ Hg^{2+}	λ SDS	λ SDS/ Hg^{2+}	ε Free	ε Hg^{2+}	ε SDS	ε SDS/ Hg^{2+}
AS1	363	359	364	367	43400	42500	46000	49000
AS2	340	304	340	304	18000	24600	16300	28600
AS3	366	315	366	315	18300	27300	17800	32500

are weaker than those of AS2 and AS3. This could be traced back to the different molecular constitutions of sensors AS1–3. In detail, for sensors AS2 and AS3 with the D–A structure, Hg^{2+}-ion complexation will significantly decrease the electron density on electron donor D and result in a depressed electron conjugation. Consequently, a distinct blue shift is observed.[17] However, for AS1, Hg^{2+}-ion complexation is expected to exert two reverse effects on its D–A–D_1 π system: 1) For the D–A part, it will result in a reduced electron conjugation and promote a spectral shift to a shorter wavelength. 2) For the D_1–A part, reduction of the electron density on the whole D–A moiety is expected to enhance the push–pull interactions between dimethylamine D_1 and the oxazole A, which facilitates a spectral shift to a longer wavelength. Thus, overall, these two effects might counterbalance each other and produce a spectral change less intensive than those of AS2 and AS3 (see reference [11] and the Supporting Information). Second, in contrast to the fluorescence spectra (see below), SDS incorporation did not initiate distinct changes in the shape of the absorption spectra during Hg^{2+}-ion addition. Third, the titration curve was steeper in the presence of SDS, thus giving a larger association constant K_s (Table 2).

Table 2. Summarized Hg^{2+}-ion association constants [M^{-1}] in the absence or presence of 12 mM SDS.

Sensor	$^1K_s/10^{5[a]}$ (no SDS)	$^2K_s/10^{5[a]}$ (SDS)	$^3K_s/10^{5[b]}$ (no SDS)	$^4K_s/10^{5[b]}$ (SDS)	$^2K_s/^1K_s$	$^4K_s/^3K_s$
AS1	4.8	18.6	3.5	22.0	3.8	6.3
AS2	4.6	17.4	2.4	16.3	3.8	6.8
AS3	3.4	16.4	1.2	10.0	4.8	8.9

[a] Determined from the absorption spectra. [b] Determined from the fluorescence spectra.

Fluorescence responses on Hg^{2+}-ion titration: Hg^{2+}-ion titration of sensor AS1 (10 μM) gradually quenched its fluorescence (Figure 3a). A chelation-enhanced quenching CHEQ[e] ($CHEQ=(I_0-I)/I_0$, I_0 and I are equal to fluorescence intensity in the absence or presence of the Hg^{2+} ion

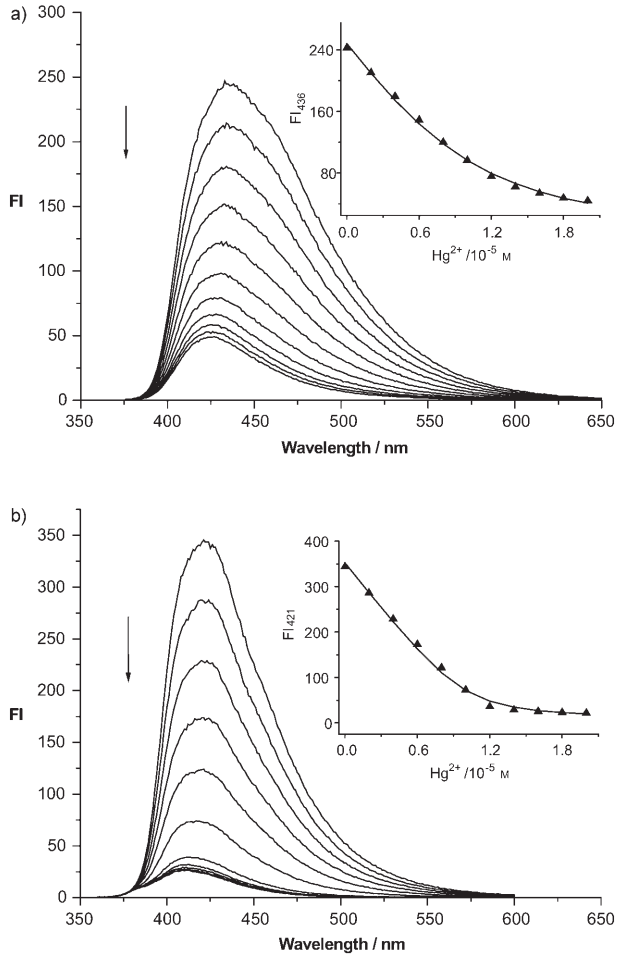

Figure 3. Hg^{2+} ion titration-induced fluorescence changes of sensor AS1 (10 μM) in the a) absence ($\lambda_{ex}=359$ nm) or b) presence ($\lambda_{ex}=346$ nm) of SDS (12 mM), in neutral water solution (pH 7.1, 25 °C). Insets: fluorescence intensity as a function of Hg^{2+}-ion concentration.

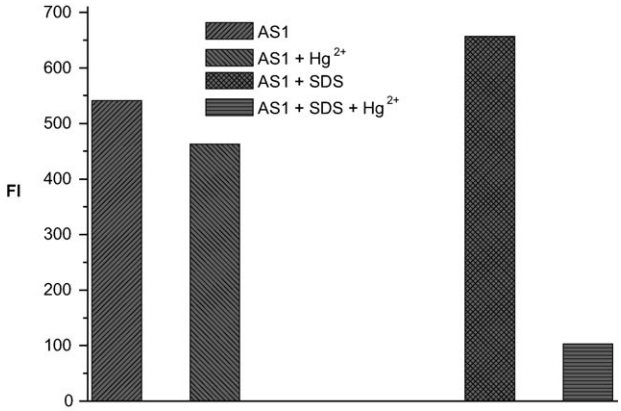

Figure 4. Hg^{2+}-ion-induced (two equivalents) fluorescence intensity changes of sensor AS1 (0.5 μM) in the absence or presence of SDS (12 mM), in neutral water solution (pH 7.1, 25 °C).

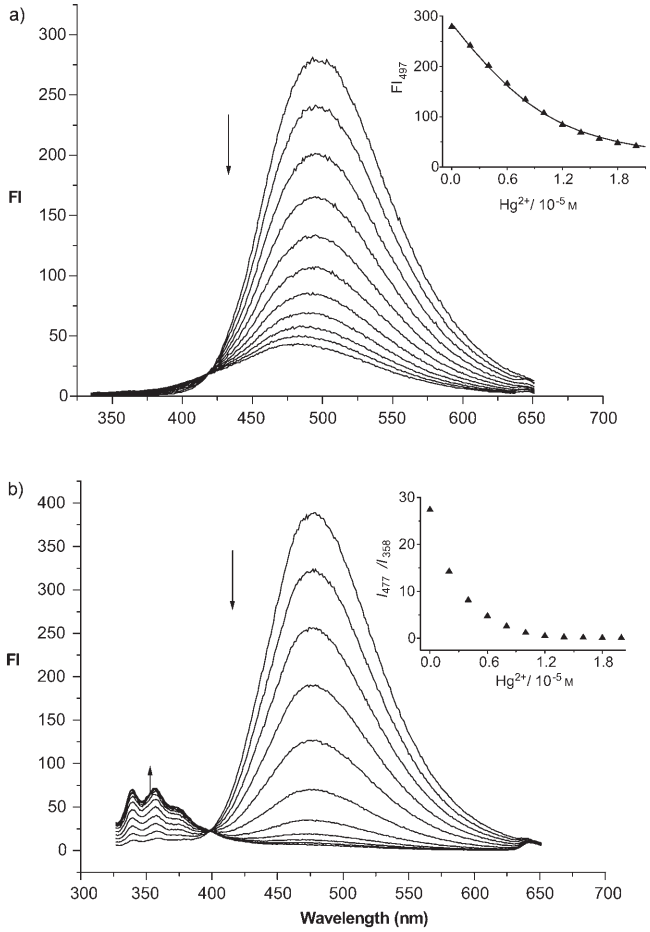

Figure 5. Hg^{2+} ion titration-induced fluorescence changes of sensor AS2 (10 μM) in the a) absence ($\lambda_{ex}=320$ nm) or b) presence ($\lambda_{ex}=320$ nm) of SDS (12 mM), in neutral water solution (pH 7.1, 25 °C). Inset: fluorescence intensity I_{497} or ratio I_{477}/I_{358} as a function of Hg^{2+}-ion concentration.

and the superscript "e" is equal to the presence of one equivalent of the Hg^{2+} ion) of 61 % was obtained. However, in the presence of 12 mM SDS, $CHEQ^e$ was increased to 79 %. Hg^{2+}-ion association[18] constants in the absence or presence of SDS were determined to be 3.5×10^5 and $22.0\times10^5\,M^{-1}$, respectively. Stronger fluorescence of the free sensor and a higher CHEQ value, together with the larger association constant, in the presence of SDS facilitate Hg^{2+}-ion detection at lower concentrations. This was clearly demonstrated by Hg^{2+}-ion titration using more dilute AS1 (0.5 μM). As shown in Figure 4, micellization significantly increased the CHEQ value from 15 to 84 % in the presence of 1 μM Hg^{2+} ions.

For sensor AS2, Hg^{2+}-ion titration in the absence of SDS exhibited similar spectral changes to those of AS1 (Figure 5a). Fluorescence at 497 nm gradually vanished with increasing Hg^{2+}-ion concentrations. A $CHEQ^e$ value of 61 % was observed. The maximum emission shifted slightly from 497 to 483 nm, producing a clear isoemissive point at 418 nm. However, the peakless emission from 340 to 418 nm was too weak to be used for ratiometric purposes. In sharp contrast, in the presence of 12 mM SDS, besides the larger $CHEQ^e$ value of 82 % at 477 nm (Figure 5b), a new well-structured emission[19] centered at 358 nm formed and devel-

oped with the gradual increasing of Hg^{2+}-ion concentration. The fluorescence intensity ratio I_{477}/I_{358} changed from 27.4 to 1.2 when one equivalent of Hg^{2+} ion was added. Clearly, SDS translated the original on–off response of AS2 toward the Hg^{2+} ion into a ratiometric signal.[20] These impressive spectral changes were preferred for practical utilization because the ratiometric signal was self-calibrated, which could largely or entirely cancel out the influences of light-source fluctuation and effective sensor concentration. Moreover, SDS significantly strengthened AS2–Hg^{2+} complexation, as could be seen from the enlarged association constant from 2.4×10^5 to $16.3\times10^5\,M^{-1}$.

For sensor AS3, SDS initiated another attractive spectrum change distinct from those of AS1 and AS2. AS3 was originally a ratiometric FSM. As shown in Figure 6a, in the absence of SDS, Hg^{2+}-ion complexation shifted the emission peak from 576 to 525 nm but no distinguishable separate emission peaks, corresponding to free AS3 and the AS3–Hg^{2+} complex, were observed during Hg^{2+}-ion titration. The fluorescence intensity ratio I_{576}/I_{525} changed from 1.5 to 0.9 in the presence of one equivalent of Hg^{2+} ion. The quantum yield decreased slightly from 0.067 to 0.062. However, in sharp contrast, Hg^{2+}-ion titration in the presence of SDS resulted in well-resolved separate emission peaks centered at 558 and 378 nm, respectively, corresponding to free AS3 and AS3–Hg^{2+} complexes (Figure 6b). Clear emission discrimination was desirable for ratiometric fluorescence molecular sensors because a strong output signal—large amplitude changes in the intensity ratio of two selected wavelengths—was expected to bring about enhanced sensitivity for analyte detection. As can be seen from AS3, the fluorescence intensity ratio I_{558}/I_{378} was changed from 22.3 to 0.31 in the presence of one equivalent of Hg^{2+} ion, which is more favorable than the counterpart "1.5 to 0.9" response obtained without SDS. The Hg^{2+}-ion association constants before and after the addition of SDS were determined to be 1.2×10^5 and $10.3\times10^5\,M^{-1}$, respectively.

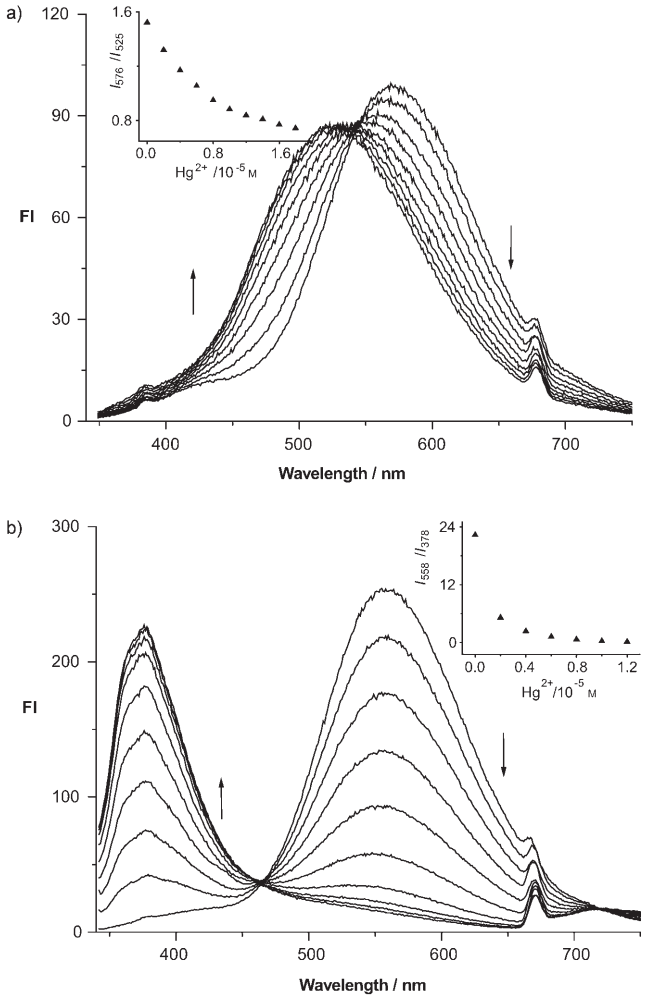

Figure 6. Hg^{2+} ion titration-induced fluorescence changes of sensor AS3 (10 μM) in the a) absence ($\lambda_{ex}=339$ nm) or b) presence ($\lambda_{ex}=339$ nm) of SDS (12 mM), in neutral water solution (pH 7.1, 25 °C). Inset: fluorescence intensity ratio I_{576}/I_{525} or I_{558}/I_{378} as a function of Hg^{2+}-ion concentration.

Discussion of the fluorescence responses of sensors AS1–3 toward the Hg^{2+} ion: Hg^{2+}-ion titration of sensors AS1–3 produces versatile fluorescence responses. Typically, 1) Hg^{2+}-ion association constants are increased substantially upon SDS addition and 2) both on–off and ratiometric signals are observed. We tentatively analyze these results based on the inherent electronic properties and the microenvironment factors of sensors AS1–3.

In detail, different substitutions of sensors AS1–3 result in different electron densities on the electron-donating 5,6-diamine nitrogen atoms, which in turn modulate the Hg^{2+} ion affinity of the tetraamide receptor.[21] For example, AS1, armed with the electron-rich dimethylamine group and containing the highest electron density on the 5,6-diamine nitrogen atoms, catches the Hg^{2+} ion more tightly and gives a higher K_s value (Table 2). As a result, the association constants decrease in line with AS1 > AS2 > AS3.

AS–Hg^{2+} complexation is notably enhanced by SDS, as demonstrated by the large ratio of ${}^2K_s/{}^1K_s$ or ${}^4K_s/{}^3K_s$. This sensitivity amplification could be attributed to the effective molarity enhancement of the Hg^{2+} ion around the negatively charged micelle surface, which promotes complexation.[7b,c,9] We noticed that association constants determined from the absorption spectra show some deviations from those determined from the fluorescence spectra (Table 2). This observation should be caused by the experimental uncertainties.[22] The absorption (steady-state fluorescence) spectra reflect the vertical transitions of a given ground (excited)-state ensemble to the corresponding Franck–Condon excited (ground) state. During these transitions, only electrons move and the nuclei are frozen. Consequently, complexes do not associate or dissociate during these processes, which means that absorption and steady-state fluorescence titrations should yield identical K_s values.[23,24]

No matter whether SDS is present, AS1 reports the Hg^{2+} ion all the time with an on–off response (Figure 4). This observation could be ascribed to the heavy-atom effect, as

tighter AS1–Hg^{2+} complexation (compared with AS2 and AS3) accelerates spin–orbit coupling and intersystem crossing, which quench the fluorescence. For AS3, Hg^{2+}-ion complexation is not expected to introduce such a strong heavy-atom effect as AS1, because the binding strength of AS3 is significantly weaker than that of AS1. Thus, AS3–Hg^{2+} complexation typically results in a wavelength shift instead of fluorescence quenching (Figure 6). However, sensor AS2, with its Hg^{2+}-ion binding strength intermediate between those of AS1 and AS3, exhibits the spectral characteristics of both the other two sensors, namely, a clearly quenched fluorescence (Figure 5a, as observed on AS1) together with a distinct spectral shift (Figure 5b, as observed on AS3).

Cation decoordination, which is commonly observed for metal-ion complexes of D–A-substituted fluoroionophores in highly polar media (see the many works of Bernard Valeur, Monique Martin, Rene Lapouyade, or Claude Rulliere), can only be operative in AS2 and AS3, but not in AS1. This explains why AS2 and AS3 show dramatic Hg^{2+}-induced shifts in absorption (see the Supporting Information Figures S7a and S8a) but only weak shifts in emission (Figures 5a and 6a). In contrast to highly polar neat aqueous solution, when the sensors are immersed in the much less polar micelles the ICT process in the excited complexes is much less promoted and clearly does not lead to cation decoordination: the complexes show well-separated blue-shifted spectra in both absorption and emission (see Figures S7b and S8b in the Supporting Information and Figures 5b and 6b). In addition, the real degree of quenching by the Hg^{2+} ion for AS2 and AS3 can only be assessed when the intrinsic fluorescence quantum yields of the parent compounds, 2-phenylbenzo[*d*]oxazole and 4-(benzo[*d*]oxazol-2-yl)benzonitrile, in the micellar medium are known.

Thermocontrolled sensitivity: Normally, a given FSM only has one dynamic detection window in which variation of the analyte concentration can be traced by its corresponding fluorescence signal. Analyte concentrations below or beyond this dynamic range (DR) are the blind spots which the sensor fails to report.[1a] Thus, it is desirable to widen the DR of a sensing system so as to monitor analyte at different concentrations, providing both qualitative and quantitative data.

The SDS–AS sensing system displays a thermocontrolled sensitivity (TCS), which could be adjusted to meet different applications. We demonstrate the principle of TCS by using AS1. As seen from Figure 7, taking advantage of the steep titration curve, sensor AS1 (0.5 μM, 25 °C) in the presence of SDS is good at indicating the Hg^{2+} ion from 0.05 to 0.9 μM. However, it is incapable of indicating Hg^{2+} ions beyond 1 μM, because the titration curve has leveled off. In sharp contrast, when the sample is heated to 68 °C, higher Hg^{2+}-ion concentrations, ranging from 1.0 to 10.0 μM, can find their corresponding fluorescence signals on the titration curve. This large-amplitude sensitivity modulation could be attributed to a temperature-induced micelle assembly and disassembly process (Scheme 3). In detail, when the temperature is low, free SDS molecules assemble into well-shaped micelles which entrap AS1 sensors and enhance their sensitivity. However, elevation of temperature increases[25] the CMC of SDS and disrupts the host micelle. As a result, the entrapped sensor molecule is again liberated into the bulk solution, in which higher concentrations of Hg^{2+} ions are needed to induce distinct fluorescence changes. We notice that elevation of temperature alone can also modulate the sensitivity.[26] On the other hand, in the absence of SDS, only a onefold enlargement of the detection window from 1.0–5.0 to 1.0–10.0 μM (the detection window is approximately estimated from the titration curve) is achieved, instead of the more than one-ordered magnification from 0.05–0.9 to 1.0–10.0 μM. Moreover, this sensitivity modulation is thermoreversible. As demonstrated by the inset of Figure 7, in the presence of two equivalents of Hg^{2+} ions, the SDS–AS1 sensing system provides two sets of fluorescence signals, corresponding to different sensitivities, when the sample is subject to alternated heating and cooling processes.

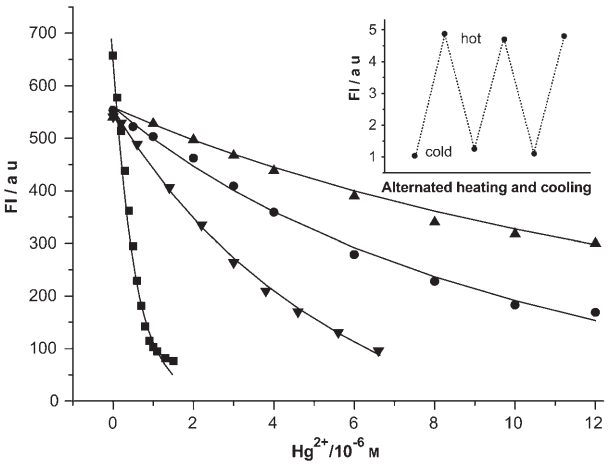

Figure 7. Temperature-controlled sensitivity of AS1 (0.5 μM) toward the Hg^{2+} ion in the absence or presence of SDS (12 mM), in neutral water solution (pH 7.1). Inset: modulating the sensitivity by alternated heating and cooling processes. ■: 25 °C, SDS; ●: 68 °C, SDS; ▲: 68 °C; ▼: 25 °C.

Scheme 3. Cartoon representation of the reversible TCS process.

Hg^{2+}-ion identification by SDS-induced fingerprint emission: In the absence of SDS, AS1–3 displayed high Hg^{2+}-ion selectivity consistent with our polyamide FSMs reported previously.[10] As demonstrated by sensor AS2, among the detected alkali-metal, alkaline-earth, transition-metal, and heavy-metal ions, Cu^{2+} and Co^{2+} induced a moderate fluorescence quenching (CHEQ[e], ≈20%) with a binding strength (for Cu^{2+}, $^{3}K_{s}=3.2\times4\,M^{-1}$, ±2%) significantly

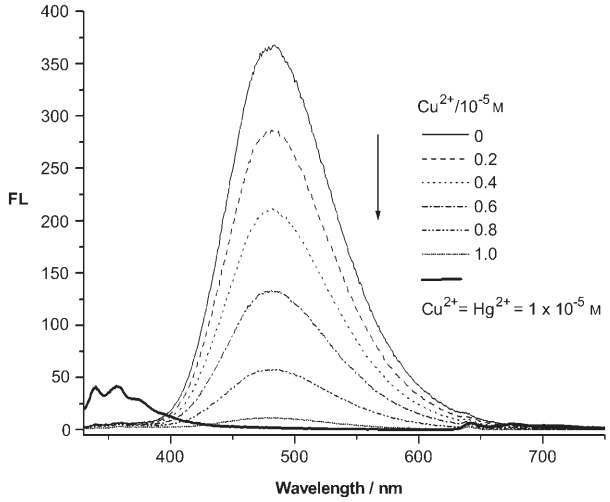

Figure 8. Cu^{2+} ion titration-induced fluorescence changes of sensor AS2 (10 μM) in the presence (λ_{ex} = 320 nm) of SDS (12 mM), in neutral water solution (pH 7.1, 25 °C). The bold line indicates the Hg^{2+}-ion identification by the fingerprint emission around 358 nm in the presence of one equivalent of Cu^{2+} ions.

weaker than that of Hg^{2+}. The other detected metal ions did not induce any detectable fluorescence response (see the Supporting Information).

In the presence of SDS, highly specific Hg^{2+}-ion identification could be achieved despite the fact that the binding strengths of AS1–3 toward Cu^{2+} and Co^{2+} were also significantly enhanced. As seen from AS2 (Figure 8), Cu^{2+} ion titration in the presence of SDS resulted in a rather high $CHEQ^e$ value of 97%,[27] but without introducing any clear emission change around 358 nm, as observed for the Hg^{2+} ion (Figure 5b). Similar spectral changes were also observed for Co^{2+} with a $CHEQ^e$ value of 89% (see the Supporting Information). Thus, in the SDS–AS2 sensing system, the short-wavelength emission around 358 nm could be assigned as the fingerprint emission of the AS2–Hg^{2+} complex, which could be used for highly specific Hg^{2+}-ion identification (Figure 9). Moreover, the Hg^{2+} ion could be indicated in the

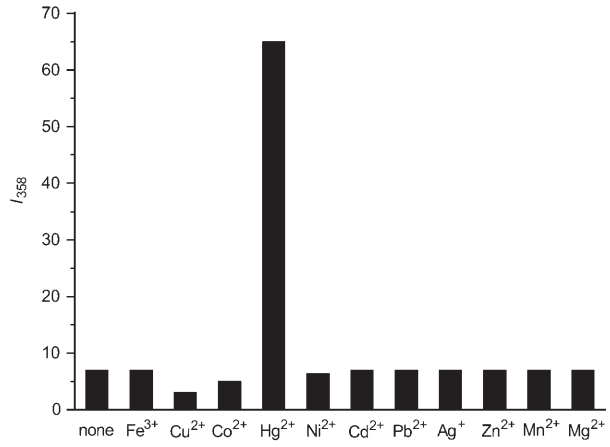

Figure 9. Metal-ion-induced (10 μM) fluorescence responses (at 358 nm) of sensor AS2 (10 μM) in the presence of SDS (12 mM), in neutral water solution (pH 7.1, 25 °C).

presence of other competing metal ions, such as Cu^{2+}. As seen from Figure 8, when Hg^{2+} ions were added to the water solution containing AS2 and Cu^{2+} ions (AS2/Hg^{2+}/Cu^{2+} 1:1:1), clear emission enhancement at 358 nm was observed. An emission ratio I_{477}/I_{358} of 0.054 was obtained, distinct from the counterpart 1.2 obtained in the "pure" AS2–Hg^{2+} sensing system (Figure 5b). Similarly, in the SDS–AS3 sensing system, the short-wavelength emission at 378 nm could also be used as the fingerprint emission of the AS3–Hg^{2+} complex. Unfortunately, it was difficult to discriminate the Hg^{2+} ion from the competing metal ions in the SDS–AS1 sensing system (see the Supporting Information).

Conclusion

A promising and convenient fluorescent molecular sensing strategy, demonstrated by the combination of anionic surfactant SDS and amphiphilic ICT Hg^{2+}-ion sensors AS1–3, is presented. This strategy displays several advantages including strengthened analyte–sensor complexation, an optimized report signal, and a thermocontrolled dynamic detection range. The success of this strategy is based on a dual "lock–key" mechanism: the first lock–key refers to the common analyte–receptor binding event, while the second lock–key refers to programming the whole sensor molecule to adapt a special microenvironment, such as the micelle, so as to fully exert its potential. We are confident that this strategy could be further extended to a wide range of sensing systems, as different microplatforms, ranging from micelle and vesicle[5] to molecular capsule[28] and dendrimer,[29] can provide microenvironments with varied polarity, rigidity, and special functional groups, which could all possibly be used to modulate the performance of a specifically fabricated fluorescent molecular sensor.

Experimental Section

General methods: All the reagents and solvents were of the highest commercial quality available and were used without purification. ^{1}H NMR spectra were recorded in $CDCl_3$ or D_2O at 25 °C on a Bruker AV-400 spectrometer. Mass spectra were recorded on a HP 1100 LC-MS spectrometer. Melting points were determined by using an X-6 micro-melting point apparatus and were uncorrected. The pH values were measured with a Sartorius basic pH-Meter PB-20. Absorption spectra were determined on a PGENERAL TU-1901 UV/Vis Spectrophotometer. Fluorescence spectroscopic studies were performed with a Hitachi F-4500

Compound 2: Compound **1** (2.23 g, 4 mmol), prepared by using the previously reported method,[10b] was dissolved in dichloromethane (10 mL), then acetic acid (100 mL) was added. $NaNO_2$ (0.69 g, 10 mmol) was added slowly to this solution over 2 min. The mixture was stirred vigorously at room temperature for 15 min, then poured into water (400 mL) and extracted twice with dichloromethane (200 mL). The combined organic phase was dried over sodium sulfate and evaporated to dryness. The residue was purified by flash chromatography using dichloromethane as the eluent, affording **2** (2.3 g, 3.92 mmol, 98%) as a yellow oil. ^{1}H NMR (400 MHz, $CDCl_3$, 25 °C): δ = 7.81 (s, 1H), 7.49 (d, J = 7.4 Hz, 2H), 7.39 (t, J = 7.4 Hz, 2H), 7.32 (t, J = 7.4 Hz, 1H), 6.67 (s, 1H), 5.16 (s,

2H), 4.40 (s, 4H), 4.15 (s, 4H), 4.14–4.10 (m, 8H), 1.24–1.20 ppm (m, 12H).

Compound 3: Compound **2** (1 g, 1.7 mmol) was dissolved in dry THF (100 mL) containing Pd/C (1 g, 5%) and cyclohexene (20 mL), and the mixture was stirred and refluxed under nitrogen for 2 h. Then the Pd/C was removed by filtration and the filtrate was concentrated under vacuum. The product was purified by flash chromatography using hexane/ethyl acetate (7:3) as the eluent, affording **3** (0.81 g, 1.63 mmol, 96%) as a red oil. ^{1}H NMR (400 MHz, $CDCl_3$, 25°C): $\delta = 10.72$ (s, 1H), 7.83 (s, 1H), 6.55 (s, 1H), 4.47 (s, 4H), 4.20–4.11 (overlapped, 12H), 1.27–1.23 ppm (m, 12H).

Compound 4: Compound **3** (0.6 g, 1.21 mmol) was dissolved in dichloromethane (5 mL) and acetic acid (50 mL). Zn powder (4 g, 62.5 mmol) was added to this solution and the mixture was stirred at room temperature for 5 min. The unreacted Zn was removed by filtration and the filtrate was poured into dichloromethane (200 mL). The organic solution was extracted three times with water (200 mL) to remove the acetic acid and dried over sodium sulfate for 5 min. Note: product **4** was not characterized because of its easy oxidation and was used directly in the following reaction.

Compound 5: 4-Dimethylaminobenzaldehyde (0.3 g, 2 mmol) was added to the above dichloromethane solution (70 mL) of compound **4** ($\approx$0.4 mmol). The solvent was evaporated under vacuum to obtain a brown oil and dry benzene (50 mL) was added. The solution was refluxed under a nitrogen atmosphere for 20 min. After this time, $BaMnO_4$ (0.31 g, 1.2 mmol) was added after slight cooling and the solution was refluxed again for another 20 min, cooled, and concentrated under vacuum. The residue was purified by flash chromatography by using hexane/ethyl acetate (7:3) as the eluent, affording **5** (0.12 g, 0.19 mmol, 48%) as a light-yellow solid. M.p. 78.2–79.6°C; ^{1}H NMR (400 MHz, $CDCl_3$, 25°C): $\delta = 8.03$ (d, $J = 8.8$ Hz, 1H), 7.39 (s, 1H), 7.28 (s, 1H), 6.76 (d, $J = 8.8$ Hz, 2H), 4.37 (s, 4H), 4.31 (s, 4H), 4.14–4.09 (m, 8H), 3.06 (s, 6H), 1.19 ppm (t, $J = 5.6$ Hz, 12H); ^{13}C NMR (100 MHz, $CDCl_3$, 25°C): $\delta = 170.9$, 164.0, 152.1, 147.0, 139.7, 139.6, 138.2, 128.7, 114.7, 111.6, 111.4, 103.3, 60.6, 60.5, 53.2, 40.1, 14.2, 14.1 ppm.

Compound 6: Compound **6** was obtained as a light-yellow solid (52%). M.p. 73.1–74.8°C; ^{1}H NMR (400 MHz, $CDCl_3$, 25°C): $\delta = 8.18$–8.16 (m, 2H), 7.50–7.49 (m, 3H), 7.47 (s, 1H), 7.34 (s, 1H), 4.39 (s, 4H), 4.33 (s, 4H), 4.15–4.09 (m, 8H), 1.22 ppm (t, $J = 5.6$ Hz, 12H); ^{13}C NMR (100 MHz, $CDCl_3$, 25°C): $\delta = 170.8$, 170.7, 162.5, 147.3, 140.9, 140.1, 137.7, 131.0, 128.8, 127.4, 127.2, 112.2, 103.6, 60.6, 60.5, 53.2, 53.1, 14.2, 14.1 ppm.

Compound 7: Compound **7** was obtained as a yellow solid (57%). M.p. 89.6–90.5°C; ^{1}H NMR (400 MHz, $CDCl_3$, 25°C): $\delta = 8.26$ (d, $J = 8.2$ Hz, 2H), 7.78 (d, $J = 8.2$ Hz, 2H), 7.50 (s, 1H), 7.34 (s, 1H), 4.41 (s, 4H), 4.34 (s, 4H), 4.15–4.10 (m, 8H), 1.21 ppm (t, $J = 7.0$ Hz, 12H); ^{13}C NMR (100 MHz, $CDCl_3$, 25°C): $\delta = 171.3$, 161.2, 148.2, 142.7, 141.2, 138.1, 133.3, 132.0, 128.1, 118.9, 114.7, 113.3, 104.2, 61.4, 61.3, 53.7, 14.8 ppm.

Sensor AS1: Compound **5** (80 mg, 0.13 mmol) was dissolved in acetonitrile (10 mL) and 2-aminoethanol (10 mL) was added. The solution was refluxed under nitrogen for 2 h, then cooled and concentrated under vacuum to remove the acetonitrile and 2-aminoethanol separately. The product was purified by flash chromatography using methanol/ammonia/dichloromethane (20:2:100) as the eluent, affording AS1 (72 mg, 0.11 mmol, 85%) as a light-yellow solid. M.p. 135.5–136.9°C; ^{1}H NMR (400 MHz, D_2O, 25°C): $\delta = 7.60$ (d, $J = 8.8$ Hz, 2H), 7.27 (s, 1H), 7.23 (s, 1H), 6.48 (br s, 2H), 4.09 (s, 4H), 4.05 (s, 4H), 3.57–3.52 (m, 8H), 3.28–3.24 (m, 8H), 2.63 ppm (s, 6H); ^{13}C NMR (100 MHz, D_2O, 25°C): $\delta =$ 172.5, 164.6, 152.5, 146.8, 140.3, 140.2, 137.1, 128.6, 112.6, 111.7, 110.5, 103.5, 59.9, 56.3, 56.2, 41.3, 41.2, 39.2 ppm; HRMS (ES+): m/z: calcd: 673.3310 [M+H$^+$]; found: 673.3315.

AS2 and AS3 were prepared similarly to AS1.

Sensor AS2: Sensor AS2 was obtained as a light-yellow solid (87%). M.p. 123.7–124.8°C; ^{1}H NMR (400 MHz, D_2O, 25°C): $\delta = 7.94$ (d, $J =$ 8.4 Hz, 2H), 7.48–7.41 (m, 3H), 7.34 (s, 1H), 7.32 (s, 1H), 4.20 (s, 4H), 4.13 (s, 4H), 3.58–3.53 (m, 8H), 3.33–3.29 ppm (m, 8H); ^{13}C NMR (100 MHz, D_2O, 25°C): $\delta = 172.5$, 163.5, 147.1, 141.1, 140.1, 136.5, 131.8, 129.0, 127.0, 125.7, 111.1, 103.6, 60.6, 55.9, 55.8, 41.3, 41.2 ppm; HRMS (ES+): m/z: calcd: 630.2888 [M+H$^+$]; found: 630.2880.

Sensor AS3: Sensor AS3 was obtained as a light-yellow solid (79%). M.p. 148.3–149.5°C; ^{1}H NMR (400 MHz, D_2O, 25°C): $\delta = 7.82$ (d, $J =$ 8.4 Hz, 2H), 7.50 (d, $J = 8.4$ Hz, 2H), 7.31 (s, 1H), 7.29 (s, 1H), 4.20 (s, 4H), 4.12 (s, 4H), 3.55–3.50 (m, 8H), 3.30–3.25 ppm (m, 8H); ^{13}C NMR (100 MHz, D_2O, 25°C): $\delta = 172.5$, 160.8, 147.1, 142.4, 141.0, 136.2, 132.6, 129.4, 126.8, 118.6, 112.9, 111.7, 103.8, 59.9, 55.7, 41.3, 41.2 ppm; HRMS (ES+): m/z: calcd [M+Na$^+$]: 677.2659; found: 677.2657.

Acknowledgements

This work was supported by the National Natural Science Foundation of China and the National Key Project for Basic Research (2003CB 114400). We thank the referees for their smart and pertinent comments; some discussions originate from their comments. We also thank Dr. A. Wu and Dr. K. Bathula for valuable discussions.

[1] For a recent book and reviews on fluorescent molecular sensors see: a) B. Valeur, *Molecular Fluorescence: Principles and Applications*, Wiley-VCH, Weinheim, **2001**; b) A. P. de Silva, H. Q. N. Gunaratne, T. Gunnlaugsson, A. J. M. Huxley, C. P. McCoy, J. T. Rademacher, T. E. Rice, *Chem. Rev.* **1997**, *97*, 1515; c) D. T. McQuade, A. E. Pullen, T. M. Swager, *Chem. Rev.* **2000**, *100*, 2537; d) R. Martínez-Máñez, F. Sancenón, *Chem. Rev.* **2003**, *103*, 4419; e) L. Pu, *Chem. Rev.* **2004**, *104*, 1687.

[2] a) K. Komatsu, K. Kikuchi, H. Kojima, Y. Urano, T. Nagano, *J. Am. Chem. Soc.* **2005**, *127*, 10197; b) E. Sasaki, H. Kojima, H. Nishimatsu, Y. Urano, K. Kikuchi, Y. Hirata, T. Nagano, *J. Am. Chem. Soc.* **2005**, *127*, 3284.

[3] C. J. Chang, J. Jaworski, E. M. Nolan, M. Sheng, S. J. Lippard, *Proc. Natl. Acad. Sci. USA* **2004**, *101*, 1129.

[4] L. Yang, R. McRae, M. M. Henary, R. Patel, B. Lai, S. Vogt, C. J. Fahrni, *Proc. Natl. Acad. Sci. USA* **2005**, *102*, 11179.

[5] D. M. Vriezema, M. C. Aragonès, J. A. A. W. Elemans, J. J. L. M. Cornelissen, A. E. Rowan, R. J. M. Nolte, *Chem. Rev.* **2005**, *105*, 1445.

[6] Y. Wan, H. Yang, D. Zhao, *Acc. Chem. Res.* **2006**, *39*, 423.

[7] Very recently, surfactants have been exploited in fluorescent molecular sensing: a) K. Niikura, E. V. Anslyn, *J. Org. Chem.* **2003**, *68*, 10156; b) A. Mallick, M. C. Mandal, B. Haldar, A. Chakrabarty, P. Das, N. Chattopadhyay, *J. Am. Chem. Soc.* **2006**, *128*, 3126; c) Y. Zhao, Z. Zhong, *Org. Lett.* **2006**, *8*, 4715.

[8] For microscopic polarity of the SDS micelle see: K. Kano, Y. Ueno, S. Hashimoto, *J. Phys. Chem.* **1985**, *89*, 3161.

[9] S. Uchiyama, G. D. McClean, K. Iwai, A. P. de Silva, *J. Am. Chem. Soc.* **2005**, *127*, 8920.

[10] We recently demonstrated that polyamide receptors could selectively bind Hg^{2+} ions in neutral aqueous solution: a) J. Wang, X. Qian, *Chem. Commun.* **2006**, 109; b) J. Wang, X. Qian, J. Cui, *J. Org. Chem.* **2006**, *71*, 4308; c) J. Wang, X. Qian, *Org. Lett.* **2006**, *8*, 3721.

[11] A closely related FSM with typical D–A–D$_1$ constitution using the benzothiazole fluorophore has been reported: K. Rurack, A. Koval'chuck, J. L. Bricks, J. L. Slominskii, *J. Am. Chem. Soc.* **2001**, *123*, 6205.

[12] Like the parent compound 2-phenylbenzoxazole, in AS1–3 the 2-phenyl ring should be electronically conjugated and coplanar with the benzoxazole moiety (energy-minimized molecular structure calculated with the Hyperchem software). This notion is supported by the ^{1}H NMR spectroscopic studies: Hg^{2+}-ion complexation results in a significant downfield shift of the aromatic protons of the 2-phenyl ring (see the Supporting Information): J. C. del Valle, M. Kasha, J. Catalán, *J. Phys. Chem. A* **1997**, *101*, 3260.

[13] A D$_1$→A transition is expected to absorb light around 350 nm, judged from the absorption of the parent chromophore 2-(4′-*N*,*N*-dimethylamino)phenylbenzoxazole: E. M. Vernigor, E. A. Lukyanets,

L. P. Savvina, V. K. Shalaev, *Chem. Heterocycl. Compd.* **1993**, *29*, 208.

[14] Determined relative to quinine sulfate: S. R. Meech, D. C. Phillips, *J. Photochem.* **1983**, *23*, 193.

[15] See reference [8]; provided that sensor incorporation does not change significantly the aggregation number (AN = 62), the micelle concentration, was calculated to be about 6×10^{-5} M in the presence of 12 mM SDS.

[16] For Hg^{2+}-ion FSMs reported in the last two years, see: a) I.-B. Kim, U. H. F. Bunz, *J. Am. Chem. Soc.* **2006**, *128*, 2818; b) Y. Zhao, Z. Zhong, *J. Am. Chem. Soc.* **2006**, *128*, 9988; c) S.-K. Ko, Y.-K. Yang, J. Tae, I. Shin, *J. Am. Chem. Soc.* **2006**, *128*, 14150; d) A. Coskun, E. U. Akkaya, *J. Am. Chem. Soc.* **2006**, *128*, 14474; e) S. Tatay, P. Gaviña, E. Coronado, E. Palomares, *Org. Lett.* **2006**, *8*, 3857; f) E. M. Nolan, M. E. Racine, S. J. Lippard, *Inorg. Chem.* **2006**, *45*, 2742; g) S. Yoon, A. E. Albers, A. P. Wong, C. J. Chang, *J. Am. Chem. Soc.* **2005**, *127*, 16030; h) A. Caballero, R. Martínez, V. Lloveras, I. Ratera, J. Vidal-Gancedo, K. Wurst, A. Tárraga, P. Molina, J. Veciana, *J. Am. Chem. Soc.* **2005**, *127*, 15666; i) E. Coronado, J. R. Galán-Mascarüs, C. Martí-Gastaldo, E. Palomares, J. R. Durrant, R. Vilar, M. Gratzel, Md. K. Nazeeruddin, *J. Am. Chem. Soc.* **2005**, *127*, 12351; j) J. V. Ros-Lis, M. D. Marcos, R. Martínez-Máñez, K. Rurack, J. Soto, *Angew. Chem.* **2005**, *117*, 4479; *Angew. Chem. Int. Ed.* **2005**, *44*, 4405.

[17] The sharp and structured absorption spectra of Hg^{2+}-ion complexes of AS2 and AS3 resembled closely, in terms of spectral shape and absorbance, that of the unsubstituted 2-phenylbenzoxazole chromophore (see the Supporting Information): D. G. Ott, F. N. Hayes, E. Hansbury, V. N. Kerr, *J. Am. Chem. Soc.* **1957**, *79*, 5448.

[18] A Job's plot indicated that AS1–3 formed a 1:1 complex with the Hg^{2+} ion, consistent with our previously reported tetraamide ICT Hg^{2+}-ion-sensor molecule (see reference [10b]).

[19] Hg^{2+}-ion complexation depresses the ICT emission and the structured fluorescence bands resemble closely that of the unsubstituted 2-phenylbenzoxazole fluorophore (see references [12] and [17]). Moreover, in a less polar acetonitrile solution, Hg^{2+}-ion titration results in emission spectra similar to that in the presence of SDS (for example, structured fluorescence band at 355 nm for AS2, see the Supporting Information).

[20] Very recently, in a Triton X-100 micelle sensing system, the fluorescence signal could by modulated by changing the lipophilicity of the receptor see: P. Pallavicini, Y. A. Diaz-Fernandez, F. Foti, C. Mangano, S. Patroni, *Chem. Eur. J.* **2007**, *13*, 178.

[21] a) S. Fery-Forgues, J. Bourson, L. Dallery, B. Valeur, *New J. Chem.* **1990**, *14*, 617; b) K. Rurack, M. Sczepan, M. Spieles, U. Resch-Genger, W. Rettig, *Chem. Phys. Lett.* **2000**, *320*, 87; c) K. Rurack, J. L. Bricks, G. Reck, R. Radeglia, U. Resch-Genger, *J. Phys. Chem. A* **2000**, *104*, 3087.

[22] The uncertainty of ${}^{1}K_{s}$ and ${}^{3}K_{s}$ is about 20% and that of ${}^{2}K_{s}$ and ${}^{4}K_{s}$ is about 40%.

[23] J. Bourson, J. Pouget, B. Valeur, *J. Phys. Chem.* **1993**, *97*, 4552.

[24] It is generally agreed that association constants larger than $4\times10^{5}\,M^{-1}$ cannot be reliably determined by conventional optical spectroscopic methods. The above discussion was initiated by the referee.

[25] B. Jönnson, B. Lindman, K. Holmberg, B. Kronberg, *Surfactants and Polymers in Aqueous Solutions*, Wiley, Chichester, **1998**.

[26] The Hg^{2+}-ion association constant was determined to be $4.8\times10^{4}\,M^{-1}\pm10\%$ at 68 °C.

[27] Cu^{2+} ion titration also initiated a distinct band shift (from 340 to 304 nm), similar to that of the Hg^{2+} ion, on the UV/visible absorption of AS2; see the Supporting Information.

[28] M. M. Conn, J. Rebek, Jr., *Chem. Rev.* **1997**, *97*, 1647.

[29] F. Zeng, S. C. Zimmerman, *Chem. Rev.* **1997**, *97*, 1681.

Received: March 20, 2007
Published online: June 21, 2007

